J Mater Sci (2007) 42:5516–5523
DOI 10.1007/s10853-006-1025-4

Strength and fracture toughness of nano and micron-silica particles bidispersed epoxy composites: evaluated by fragility parameter

Soon-Chul Kwon · Tadaharu Adachi

Received: 19 July 2006 / Accepted: 25 September 2006 / Published online: 3 April 2007

Abstract In this study, we discuss the composition effect of 240 nm and 1.56 μm-silica particles on strength and fracture toughness by examining two parameters, fragility and glass transition temperature, that were derived from the thermo-viscoelasticity measurements. Experimental results showed that the composites had a lower fragility with higher strength and fracture toughness as the content of nanoparticles was increased regardless of glass transition temperature. The improvement in mechanical properties from adding nanoparticles was definitely explained by the fragility represented the heterogeneity in polymer matrix, and this was related to the interaction between particles and matrix. The fragility was found to be an effective parameter for evaluating strength and fracture toughness of epoxy composite containing a bidispersion of nano and micron-silica particles.

Introduction

The mechanical properties of particulate-filled composites, such as strength, fracture toughness and thermo-viscoelasticity, have been remarkably improved by the reduction of the particle size. Kinloch et al. [1, 2] and Huang et al. [3] found that the thermal and mechanical properties of the epoxy-matrix composites had different dependences on particle sizes. Furthermore, a rapid decrease in the inter-particle distance resulting from their small size in turn resulted in more interactions between particles and epoxy matrix.

For a particulate structure, the interfacial interaction of particles with the surrounding matrix has a close relation with the cross-linking network morphology in the polymer matrix [4–6]. As a result, the mechanical properties of the nano or micron-particles reinforced epoxy composites were considerably dependent not only on the particle size effect but also on the intrinsic properties of the epoxy matrix.

Glass transition temperature, T_g was regarded as the most important parameter for evaluating the mechanical properties of the polymers and the polymer-matrix composites because T_g was generally represented as the degree of cross-linking of polymer materials. Other researchers [7–9] found that the thermal and mechanical properties of the epoxy composites were increased while the T_g decreased. However, Wu et al. [10] and Araki et al. [11] reported that the fracture toughness of the epoxies was increased while the saturated cross-linking density preserved T_g at constant value.

The fragility parameter, m was originally introduced by Angell [12]. As a useful means of representing the density of heterogeneity at various amorphous materials, the concept of fragility has been widely applied in characterizing the cross-linked polymers [13, 14] and the glass-forming liquids [15, 16]. Kanaya et al. [17, 18] reported the relative dependency of heterogeneity on fragility in the amorphous polymers based on incoherent elastic scattering data. Adachi et al. [19] found that the fracture toughness of the silica particle monodispersed epoxy composites was obviously dependent on fragility.

In this study, we discuss the composition effect of 240 nm and 1.56 μm-silica particles on strength and fracture toughness by examining two parameters: fragility and

S.-C. Kwon · T. Adachi (✉)
Department of Mechanical Sciences and Engineering,
Tokyo Institute of Technology, 2-12-1 O-okayama, Meguro-ku,
Tokyo 152-8552, Japan
e-mail: adachi@mech.titech.ac.jp

glass transition temperature. The purpose is to suggest an effective parameter for clarifying the effect of particle size in characterization of mechanical properties based on the correlation between these two parameters and both strength and fracture toughness.

Experimental

Materials and specimen preparation

The materials of specimen used in this study were bisphenol A-type epoxy composites reinforced by spherical silica particles. The specimens had different particle size compositions but the same constant total volume fraction of filled particles, 0.30.

The matrix was mixed from bisphenol-A type epoxide resin (Epikote 828, Japan Epoxy Resins), a hardener of methyltetrahydro-phthalic anhydride (HN-2200R, Hitachi Chemical), and an accelerator of 2,4,6-Tris (dimethyl amino-methyl) phenol (DMP 30, Kayaku Akuzo) in proportions of 100:80:0.5 by weight.

Figure 1 shows two types of the fused spherical silica particles filled in epoxy matrix. The median diameter, D_m of each particle was measured as 240 nm for 1-FX (Tatsumori Ltd.) and 1.56 μm for SO-C5 (Tatsumori Ltd.), respectively. Both particles had a similar particle distribution as shown in Fig. 2. Surfaces of the particles were not chemically treated.

Five types of the specimens of the silica particulate-filled epoxy composite were prepared where the total particles volume fraction, V_P, was constantly fixed at 0.30,

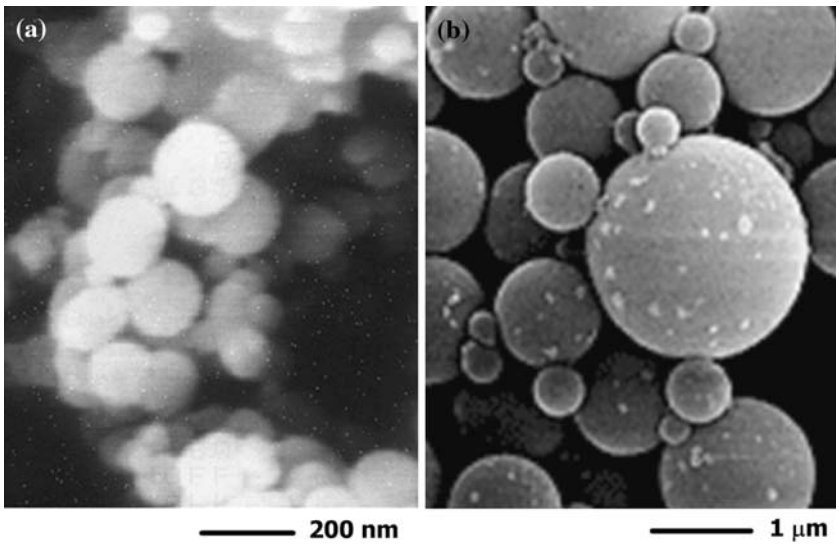

Fig. 1 Fused spherical silica particles (**a**) nano-particle, 1-FX; (**b**) micron-particle, SO-C5

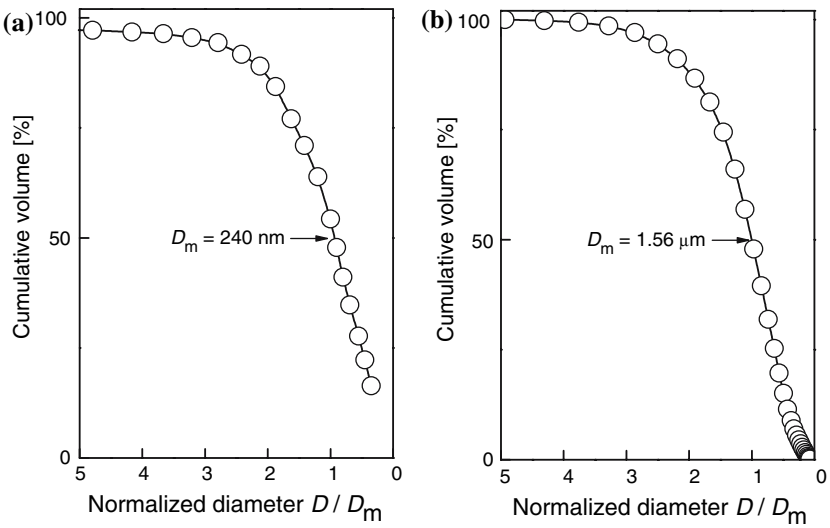

Fig. 2 Normalized silica particle size distributions (**a**) nano-particle, 1-FX; (**b**) micron-particle, SO-C5

Table 1 Silica/epoxy composites with various particle compositions

Composition ratio Φ_{SP}	Ratio of nano and micron-particle content 1-FX / SO-C5 [wt% / wt%]	Total volume fraction V_p
0	0 / 100	0.30
0.2	20 / 80	0.30
0.5	50 / 50	0.30
0.8	80 / 20	0.30
1.0	100 / 0	0.30

while the applied composition ratio of two-silica-particle, Φ_{SP}, defined as the weight fraction of 1-FX particles to the total particles, ranged from 0 to 1.0, as listed in Table 1.

The mixed particles were completely dispersed into the epoxy resin during blending and degassing processes: the silica particles were compounded into a blend of epoxy resin, hardener, and accelerator with a mixing machine (Retsch, KM100) until any cohesion of particles disappeared in the matrix resin (about 30–60 min, room temperature). Subsequently, its mixtures were poured into a Teflon-coated mold made from aluminum alloy after being fully agitated and degassed by vacuum process. The mold was 260 mm long, 5 mm wide, and 180 mm deep, respectively.

After inspecting of the particle distribution by micrograph, the cured composite plates were cut into specimens with proper dimensions and shapes for each test. Furthermore, if the voids or the particle agglomeration in fracture surfaces were observed by SEM after each test, its experimental data was excluded from the final results of this study.

The curing of each composite was performed using the same steps. In pre-curing, the specimen was first kept at 353 K for 3 h to gel the epoxy resin. Then, in post-curing, which greatly affects the cross-linking reaction of the epoxy, the specimen was cured for 15 h at 413 K. For comparison, neat epoxy without any particles was also prepared and cured using the same process described above.

Thermo-viscoelasticity measurement

Experimental procedure

The thermo-viscoelastic properties of the neat epoxy and the composites were measured with a dynamic viscoelastometer (Orientec, Rheovibron DDV-III-EA) by using the nonresonance tensile method. The specimens were 5 mm wide by 2 mm thick and 70 mm long.

The storage modulus E', loss modulus E'' and tan δ ($=E''/E'$) were measured at each temperature interval of 2 K in the range from 123 K to 523 K with a 1.5 K/min heating rate by applying the tensile oscillations at frequencies of 3.5, 11, 35, and 110 Hz.

Glass transition temperature

The master curves for each of the neat epoxy and the composites were derived from the E' measured at each temperature according to time–temperature equivalence principle. The E' measured at different temperatures were shifted horizontally to the modulus at the reference temperature along the frequency f axis, hence the master curve could be plotted by a shift factor, α_T, defined as the amount of time ($1/f$) shift for each temperature. For typical examples, Figs. 3 and 4 show measured E' curves at 10 K temperature increments and the master curves for the neat epoxy and the composite of the particle composition ratio, Φ_{SP} = 0.8, respectively.

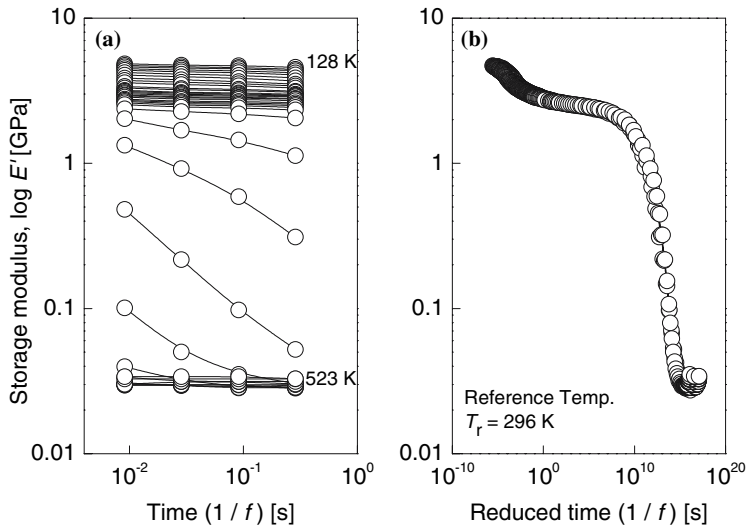

Fig. 3 Storage modulus of neat epoxy (**a**) measured at 10 K temperature increments; (**b**) master curve

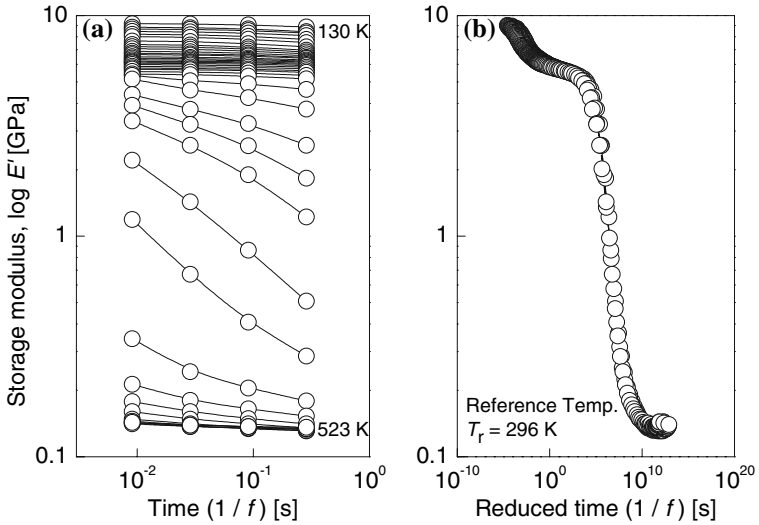

Fig. 4 Storage modulus of composite with $\Phi_{SP} = 0.8$ (**a**) measured at 10 K temperature increments; (**b**) master curve

The shift factor, α_T, as a function of temperature is governed by the thermal activation process, and can be expressed as an Arrhenius equation [20]:

$$\log \alpha_T = \frac{\Delta H}{R}\left(\frac{1}{T} - \frac{1}{T_r}\right) \tag{1}$$

where T, T_r, R, and ΔH are the absolute temperature, the reference temperature, the universal gas constant (=8.314 J/mol·K), and the apparent activation energy, respectively.

Although the glass transition temperature, T_g was simply determined from the tan δ peak of the thermo-viscoelasticity at 3.5 Hz oscillation in [21], the T_g used in this study were defined as a temperature corresponding to the maximum value of ΔH in Eq. (1) [19, 22, 23].

Fragility

Angell [12] proposed the fragility m, defined as the slope at $T = T_g$ of the temperature-dependent relaxation time, τ, in an Arrhenius plot [16] as follows:

$$m = \left.\frac{d(\log \tau)}{d(T_g/T)}\right|_{T=T_g} \tag{2}$$

The neat epoxy and the composites are known as a themorheologically simple material [24, 25], then the shift factor, α_T can be expressed as follows [26]:

$$\alpha_T = \frac{\tau(T)}{\tau(T_r)} \tag{3}$$

Substituting Eq. (3) into Eq. (2), fragility m can be defined by the following expression [19, 22, 23]:

$$m = \left.\frac{d(\log \alpha_T)}{d(T_g/T)}\right|_{T=T_g} \tag{4}$$

Hence, the value of m was determined from the slope of α_T with the reciprocal of the temperature normalized by T_g.

Mechanical properties measurements

Bending strength

The bending strength, σ_B for both the neat epoxy and the composites were determined at the maximum load where brittle breaking occurred. The tests were carried out at 296 K with a deformation rate of 44.8 μm/s using a universal testing machine (Instron 8501), according to ASTM standard D 790-03. The specimens were 15 mm wide by 5 mm thick and 100 mm long, and the span length between the supports was 80 mm.

Fracture toughness

Single edge notched bending tests were performed to measure the mode I fracture toughness of the neat epoxy and the composites in terms of the critical stress intensity factor K_{IC}, according to ASTM standard D 5045-91. The specimens were 5 mm wide by 20 mm thick and 90 mm long. A slot notch was created 9 mm in depth by sawing, and a sharp crack was initiated by a razor blade into the notch with 1 mm deep. Every experiment was carried out at 296 K using a universal testing machine (Instron 8501) with a constant crosshead speed of 2.0 μm/s.

The load–deflection curves of all specimens were linear until brittle breaking occurred, specifically the stress field near the crack tip was small scale yielding. Then, the

fracture toughness, K_{IC} was calculated by using the linear elastic fracture mechanics [27].

$$K_{IC} = \frac{SP_C}{BW^{3/2}} f(\xi) \tag{5}$$

where

$$f(\xi) = \frac{3\xi^{1/2}\left[1.99 - \xi(1-\xi)(2.15 - 3.93\xi + 2.7\xi^2)\right]}{2(1+2\xi)(1-\xi)^{3/2}},$$

$$\xi = \frac{a_0}{W}$$

S and P_C are the span length and the maximum load, and B, W, and a_0 are the thickness, width and pre-crack length of the specimen.

Experimental results

Glass transition temperature and fragility

Figure 5 shows the dependence of T_g on the composition ratio of particles, Φ_{SP}, for the neat epoxy and the composites. The T_g of all composites was roughly the same since the cross-linking reaction saturated, but peaked slightly at the composite with Φ_{SP} = 0.5 and approximately 2 K lower than that of the neat epoxy. This variation of T_g with Φ_{SP} implied the relation with packing particles in matrix. When the cross-linking degree of the composites saturated, as discussed in previous study [21], the degree of particle packing obviously affected the thermo-viscoelastic properties of the composites. Generally, smaller particles were easily able to interpose between large particles, especially in a proper bidispersion of particles.

The Arrhenius plots of log α_T with the reciprocal of normalized temperature by T_g obtained from the master curves of the neat epoxy and the composites are shown in Fig. 6. The results showed the relatively small slopes of the composites compared with that of the neat epoxy. The log α_T slopes, namely fragilities m, for the neat epoxy and the composites are shown in Fig. 7. The m of the composites monotonically decreased with Φ_{SP} and had different tendency than the T_g-Φ_{SP} relation. The composite with Φ_{SP} = 1.0 showed the m of 42 that decreased 33 % compared to the m of 63 at Φ_{SP} = 0. This definitely indicated that the fragility of the composites was not be directly related to the geometrical packing particles in matrix. An increase in Φ_{SP} was correlated to a decrease in interspaces between adjacent particles [21]. In addition, a decrease in fragility represented increasing the heterogeneity in the polymer matrix. Therefore, the result of decreasing m with high Φ_{SP} showed the relationship between the heterogeneity in epoxy matrix and the interparticle distance.

Strength and fracture toughness

The experimental results of σ_B and K_{IC} for the neat epoxy and the composites measured at 296 K are presented in Figs. 8 and 9, respectively. Compared with the lowest σ_B and K_{IC} of the neat epoxy measured as 127.6 MPa and 0.97 MPa·m$^{1/2}$, σ_B of the composites increased from 135.8 MPa of Φ_{SP} = 0 to 171.2 MPa of Φ_{SP} = 1.0. For the K_{IC}, the

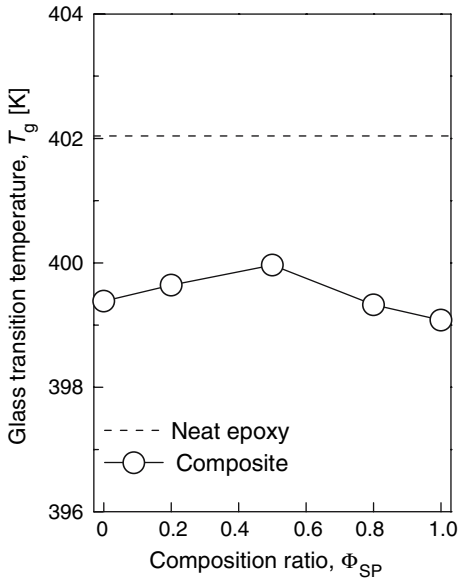

Fig. 5 Particle composition dependence of glass transition temperature

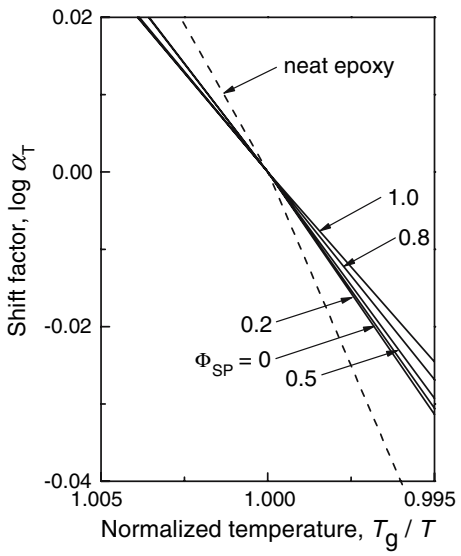

Fig. 6 Arrhenius plots of shift factor: Referenced temperature, $T_r = T_g$ = 296 K

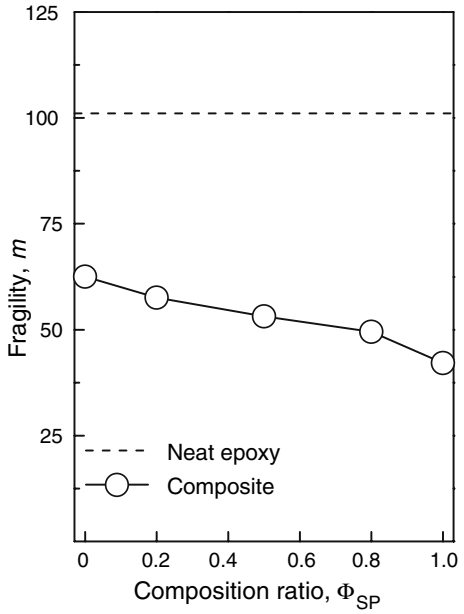

Fig. 7 Dependence of fragility on particle composition

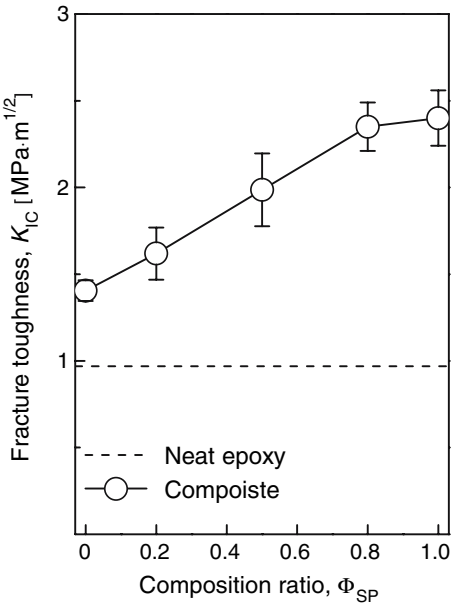

Fig. 9 Fracture toughnesses of neat epoxy and composites

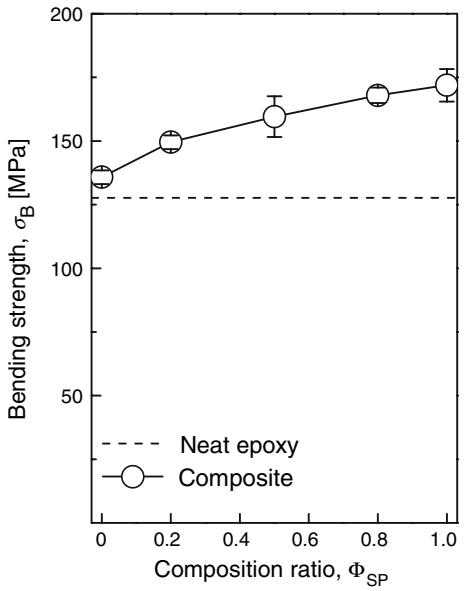

Fig. 8 Bending strengths of neat epoxy and composites

composite with $\Phi_{SP} = 1.0$ had the highest, 2.41 MPa·m$^{1/2}$ more than the 1.40 MPa·m$^{1/2}$ of the composite of $\Phi_{SP} = 0$. Thus, these properties of the composites were significantly dependent on Φ_{SP}.

Discussion

Figure 10 shows the relations between T_g and both σ_B and K_{IC} for the neat epoxy and the composites. We plotted the measured properties as the average values with error bars denoting the standard deviation of the experimental data. As shown in the figures, the strength and fracture toughness of the composites varied regardless of T_g. This is because the T_g of the composites was strongly dependent on the degree of particle packing and was not directly dependent on the composition ratio of particles Φ_{SP}, as discussed in [21].

The σ_B and K_{IC} of the composites showed a distinct relation with the fragility, as shown in Fig. 11. The properties were plotted as the average values with errors bar denoting the standard deviation of the experimental data. The σ_B and K_{IC} of the composites increased as the m monotonically decreased. The composite with $\Phi_{SP} = 1.0$ had higher properties with the lowest m.

Based on the experimental results and the crack propagation in a matrix [28], we concluded that the strength and fracture toughness of the composites were governed by the epoxy matrix properties expressed as fragility. The strength and fracture toughness could not always be attributed to the stress field in the matrix that depended on the elastic and dynamic moduli concerning particle packing with a constant particle volume [21]. When the content of smaller particles increased, this narrowed the interparticle distance and led to inducing heterogeneity in the epoxy matrix by increasing the particle-matrix interactions. Therefore, this heterogeneity should strengthen and toughen the epoxy matrix, finally causing high strength and fracture toughness of the composites. In the case of the addition of nanoparticles, much higher mechanical properties of the composites could be explained by attributing this to the

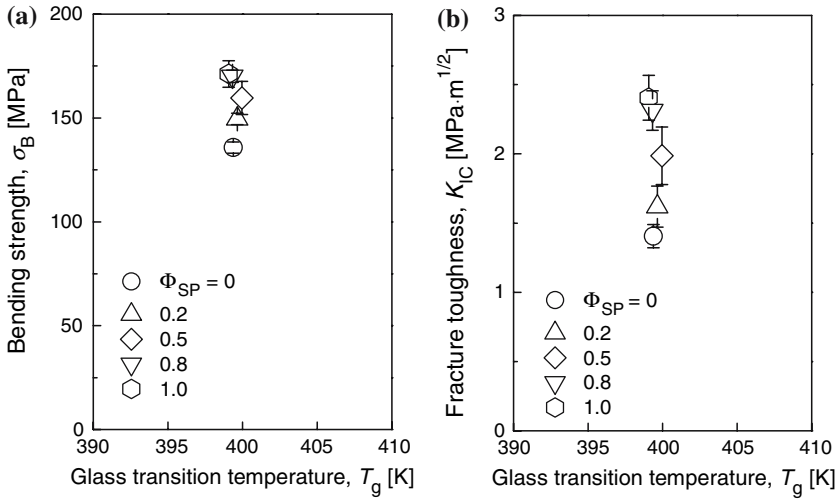

Fig. 10 Relation between glass transition temperature and mechanical properties (**a**) strength; (**b**) fracture toughness

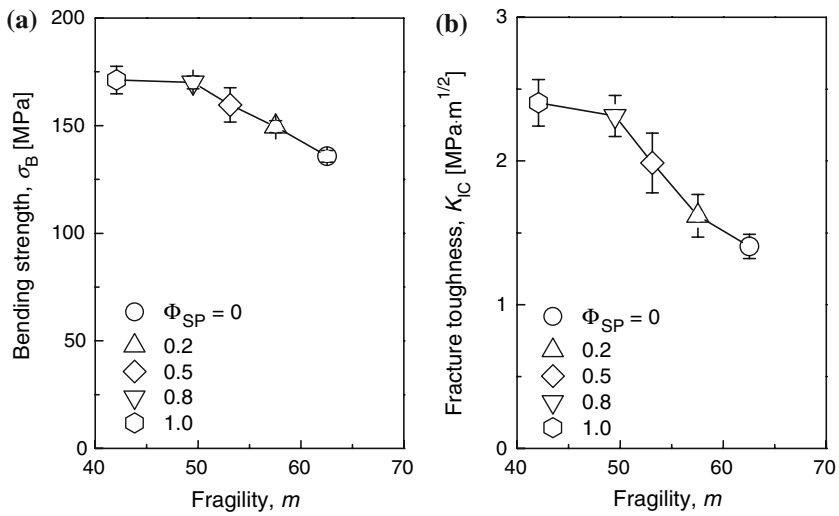

Fig. 11 Relation between fragility and mechanical properties (**a**) strength; (**b**) fracture toughness

heterogeneity expressed by fragility due to more interactions between nanoparticles and polymer matrix.

Conclusion

In this study, we discussed the composition effect of 240 nm and 1.56 μm-silica particles on strength and fracture toughness by examining two parameters: fragility and glass transition temperature. Five types of specimens with various two-particle composition ratios were prepared where the total particles volume fraction was constantly fixed at 0.30.

An increase in the content of nanoparticles gave rise to not only an increase in the strength and fracture toughness but also a decrease in the fragility of the composites. However, simultaneously, these mechanical properties increased regardless of glass transition temperature. The reduction in interparticle distance caused the particle-matrix interactions to induce heterogeneity in the matrix expressed as decreasing fragility. Then epoxy matrix toughened by this heterogeneity would ultimately improve the strength and fracture toughness of the composites.

Fragility was found to be effective parameter for evaluating strength and fracture toughness of epoxy composite having bidispersion of nano and micron-silica particles. Moreover, the effect of nanoparticles on these properties was also effectively explained using the fragility discussed in this study.

References

1. Kinloch AJ, Taylor AC (2003) J Mater Sci Lett 22:1439
2. Kinloch AJ, Lee JH, Taylor AC, Sprenger S, Eger C, Egan D (2003) J Adhesion 79:867
3. Huang KS, Nien YH, Chen JS, Shieh TR, Chen JW (2006) Polym Compos 27:195
4. Rong MZ, Zhang MQ, Pan SL, Lehmann B, Friedrich K (2004) Polym Int 53:176

5. Brechet Y, Cavaille J-YY, Chabert E, Chazeau L, Dendievel R, Flandin L, Gauthier C (2001) Adv Eng Mater 3:571
6. Kovacevic V, Lucic S, Leskovac M (2002) J Adhesion Sci 16:1343
7. Park JH, Jana SC (2003) Polymer 44:2091
8. Nikkeshi S, Kudo M, Masuko T (1998) J Appl Polym Sci 69:2593
9. Miyagawa H, Rich MJ, Drzal LT (2005) Polym Compos 26:42
10. Wu WL, Hu JT, Hunston DL (1990) Polym Eng Sci 30:835
11. Araki W, Adachi T, Yamaji A (2006) Recent Res Dev Appl Polym Sci 3:205
12. Angell CA (1988) J Phys Chem Solid 49:863
13. Matsuoka S, Quan X, Bair HE, Boyle DJ (1989) Macromolecules 22:4093
14. Racich JL, Koutsky JA (1976) J Appl Polym Sci 20:2111
15. Si P, Bian X, Zhang J, Li H, Sun M, Zhao Y (2003) J Phys Condens Matter 15:5409
16. Böhmer R, Ngai KL, Angell CA, Plazek DJ (1993) J Chem Phys 99:4201
17. Kanaya T, Kawaguchi T, Kaji K (1996) J Chem Phys 104:3841
18. Kanaya T, Tsukushi I, Kaji K (1997) Prog Theoret Phys Suppl 126:133
19. Adachi T, Araki W, Nakahara T, Yamaji A, Gamou M (2002) J Appl Polym Sci 86:2261
20. Nielsen LE, Landel RF (1994) Mechanical properties of polymers and composites. Marcel Dekker, New York, p 131
21. Kwon S-C, Adachi T, Araki W, Yamaji A (2006) Acta Mater 54:3369
22. Araki W, Adachi T, Yamaji A, Gamou M (2002) J Appl Polym Sci 86:2266
23. Araki W, Adachi T, Yamaji A (2003) JSME Int J 46:163
24. Plazek DJ, Choy IC (1989) J Polym Sci Pt 27:307
25. Plazek DJ, Choy IC, Kelley FN, Meerwall E, Suş LJ (1982) Rubber Chem Tech 56:866
26. Schwarzl F, Staverman AJ (1952) J Appl Phys 23:838
27. Benthem JP, Koiter WT (1975) In: Mechanical fracture, vol. 1 Methods of analysis and solutions of crack problems. Noordhoff International Publishing, Leyden
28. Kwon S-C, Adachi T, Araki W, Yamaji A (2005) Key Eng Mat 297–300:207